Forward Osmosis Desalination Using Thermoresponsive Hydrogels as Draw Agents;

An Experimental Study

by

Adnan Abdullahi

A Thesis Presented in Partial Fulfillment
of the Requirements for the Degree
Master of Science

Approved April 2019 by the
Graduate Supervisory Committee:

Patrick Phelan, Chair
Lenore Dai
Robert Wang

ARIZONA STATE UNIVERSITY

May 2019

ABSTRACT

Hydrogel polymers have been the subject of many studies, due to their fascinating ability to alternate between being hydrophilic and hydrophobic, upon the application of appropriate stimuli. In particular, thermo-responsive hydrogels such as N-Isopropylacrylamide (NIPAM), which possess a unique lower critical solution temperature (LCST) of 32°C, have been leveraged for membrane-based processes such as using NIPAM as a draw agent for forward osmosis (FO) desalination. The low LCST temperature of NIPAM ensures that fresh water can be recovered, at a modest energy cost as compared to other thermally based desalination processes which require water recovery at higher temperatures. This work studies by experimentation, key process parameters involved in desalination by FO using NIPAM and a copolymer of NIPAM and Sodium Acrylate (NIPAM-SA). It encompasses synthesis of the hydrogels, development of experiments to effectively characterize synthesized products, and the measuring of FO performance for the individual hydrogels. FO performance was measured using single layers of NIPAM and NIPAM-SA respectively. The values of permeation flux obtained were compared to relevant published literature and it was found to be within reasonable range. Furthermore, a conceptual design for future large-scale implementation of this technology is proposed. It is proposed that perhaps more effort should focus on physical processes that have the ability to increase the low permeation flux of hydrogel driven FO desalination systems, rather than development of novel classes of hydrogels.

ACKNOWLEDGMENTS

This work would not have been possible without support from numerous individuals, chief among which is my advisor and committee chair Dr Patrick Phelan. Likewise, I would like to thank Dr Praveen Kumar, Roshan Sameer Annam and Hooman Daghooghi for their unique roles in the beginning and throughout the entire journey of this work. Finally, I would like to thank the Mastercard Foundation Scholarship program for funding my academic endeavors and providing me with opportunities to fulfill my potentials.

DEDICATION

Dedicated to anyone in the tireless pursuit of excellence and truth!

TABLE OF CONTENTS

Page

LIST OF FIGURES

Figure Page

Figure Page

NOMENCLATURE

LCST	Lower Critical Solution Temperature
FO	Forward Osmosis
RO	Reverse Osmosis
NIPAM	N-isopropylacrylamide
SA	Sodium Acrylate
ppm	Parts per million
M_s	Mass of swollen hydrogel
M_D	Mass of dry hydrogel
ΔH_C	Absorbing heat for apolar dehydration
ΔH_{hg}	Absorbing heat for polar dehydration
ΔH_{trans}	Transition heat of collapse

CHAPTER ONE

INTRODUCTION

1.1 State of The World's Water Resources and Need for Desalination

Perhaps the most critical natural resource on earth, for which man's survival is inextricably linked to, is water. Water as a resource, is of a paradoxical nature, as its abundant yet scarce nature can be said to exist simultaneously. Although more than 70% of the earth's surface is covered by water, 97% of the water remains unavailable to man due to its salt content [1]. Harnessing this vast amount of water by desalination has been studied to great extent, and owing to these studies, current technologies exist that allow fresh water to be tapped from the available salty water. The national Academy of Engineers (NAE), a global reputable body, rightly lists as part of its 14 grand engineering challenges, the challenge of providing access to clean water. This is in recognition of the primacy of water and the enormity of the challenge that faces mankind if more of earth's water resources are not able to be tapped into sustainably and at lower energy costs than what is the norm today. To solve the challenge of water insecurity, scientists and engineers pursuing viable solutions can be classified into two main groups. The first group advocates for an approach that seeks to optimize the use of current water resources through recycling water and developing strategies for promoting reduced water use. The second group, for which this work may also be classified under, favors the development of more efficient and less expensive desalination methods. It is evident though, that no one approach can on its own solve the entirety of the world's water challenge, and both groups need to trail their individual paths, for the benefit of the world.

1.2 Current Desalination State of The Art

Desalination is currently achieved by either thermal approaches such as; Multi stage Flash distillation (MFD), Multi Effect Distillation (MED), and Mechanical Vapor compression, or by membrane-based processes such as Sea Water reverse osmosis, Brackish water reverse osmosis and more relevant to this work, forward osmosis [2]. Membrane-based desalination processes as the name implies, require the key use of a semi permeable membrane material to effect desalination. On the other hand, thermal approaches to desalination rely heavily on thermal energy input to evaporate and condense sea water.

Currently, thermal-based desalination processes require 7-14 kWh/m^3 while membrane-based processes require 2-6 kWh/m^3 to achieve seawater desalination [4]. Amongst the membrane based processed, RO is the most popular and remains indispensable amongst membrane desalination options. However, RO has drawbacks, some of which include membrane fouling and high operating pressure requirements at low water recovery [4]. Engineers and scientists globally are continually dedicating time and resources to reducing both the cost of, and energy intake of both thermal and membrane-based desalination systems. Given the enormity of the task of attaining global water security, it is crucial that any long-term solution be as energy efficient as possible

1.3 Forward Osmosis and Issues with Current Draw Agents

Literature is conscious to note that Forward Osmosis (FO) is an emerging technology that on its own has not yet found commercial use. Although FO can be used to achieve direct desalination, the energy required to recover conventional FO related draw agents, hinders this application. Indirect desalination, where salt water is used as the draw agent, and low-quality water as the feed is a field where FO has found its niche. This coupled with a low-pressure RO system does not require a pressure gradient and can achieve desalination at lower energy costs [5]. FO works by extracting water from a lower osmotic pressure saline feed supply through a semi permeable membrane to a higher osmotic pressure draw agent [5]. The now diluted draw agent must be recovered via an additional thermal process, that allows for both recovery of draw agent and separated water.

Draw agents are key to FO, as they can be said to play a similar role to pumps in RO processes. The suitability of numerous conventional draw agents has been investigated in literature for use in FO direct desalination systems. However due to issues regarding recovery of the draw agents at low energy costs, and concerns regarding the portability of water produced using these draw agents, their use has been limited [6]. For example, ammonium bicarbonate, a thermolytic ammonium salt which has been shown to generate sufficient water flux, has been reported to require recovery at a temperature approaching 60℃ and also comes with the additional drawback of difficulty in completely separating it from the fresh water, resulting in quality impaired water been recovered [6]. This has led to the investigation of alternative draw agents, which require lower energy to recover, and do not mar the quality of water or lead to membrane fouling,

1.4 Overview of Hydrogels and Their Suitability as Draw Agents

Hydrogels have been defined in a plethora of ways by researchers and chemists. Perhaps, one definition that truly captures the essence and functionality of this class of materials is the definition that describes hydrogels as – a polymeric material that exhibits the ability to swell in water and retain a significant amount of water in its structure but will not itself dissolve in water [7]. Hydrogels as a class of materials inherently posses a dual nature. They can behave as both hydrophobic and hydrophilic materials, upon the application of an appropriate stimuli. It is worthwhile to note that hydrogels refer to a class/group of materials and not a single material.

Switching from a hydrophilic state to a hydrophobic state by hydrogels is usually achieved by the application of a stimulus. Different types of hydrogels have different types of stimuli to which they best respond. Figure 1 shows some examples of both physical and chemical stimuli that would elicit a response from the hydrogel and force it to transition from being hydrophilic to hydrophobic.

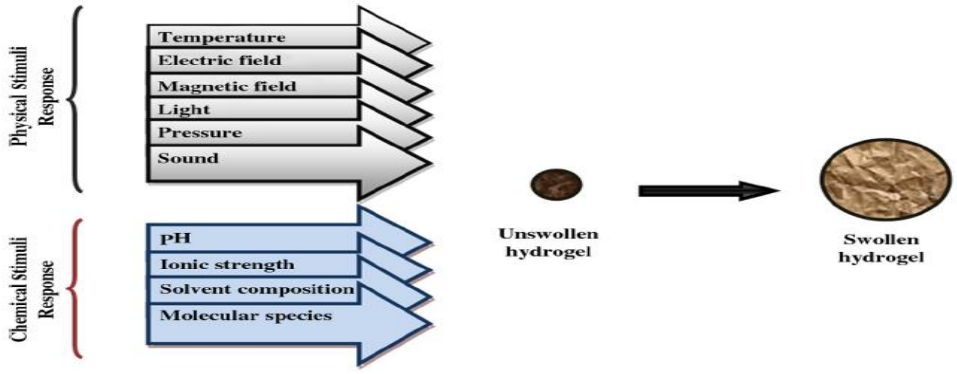

Figure 1; A schematic of various stimuli that can cause a reversible volume transition in hydrogels. [8]

N-isopropylacrylamide (NIPAM) is a class of hydrogels that undergoes a volume phase transition upon the application of a temperature stimulus. Literature reports that the LCST of NIPAM is around 32℃, which is the temperature required to force NIPAM to change from being hydrophilic to hydrophobic [6]. This is evidently a huge leap from the thermal decomposition temperature required to regenerate a conventional draw agent like ammonium bicarbonate. That is coupled with the facts that NIPAM presents little or no fouling to FO membranes, is devoid of issues concerning quality of retrieved water, and does not come with the high reverse diffusion of a salt like ammonium bicarbonate [6].

Razmjou et al. (2013) demonstrated that thermoresponsive hydrogels, particularly NIPAM, can generate enough osmotic pressure to serve as a draw agent for FO desalination. The high swelling ratio of NIPAM coupled with the fact that the water drawn through a membrane from a saline feed solution can be released at relatively low temperature cost, with NIPAM regaining its shape and volume, makes NIPAM an attractive draw agent [6]. Furthermore, Amir et al. demonstrated that incorporating a hydrophilic ionic compound to NIPAM, such as sodium acrylate (SA) increases the osmotic pressure generatable but at the expense of a significant increase in LCST of the new compound. Literature reports that a compound generated by the copolymerization of NIPAM and SA would possess an LCST of about 80℃ [7].

CHAPTER 2

SYNTHESIS AND CHARACTERIZATION EXPERIMENTS

2.1 First Synthesis and Setup of Synthesis Environment

Hydrogels can be synthesized by a number of ways, as reported by literature. For this work, both Thermoresponsive hydrogels, NIPAM and NIPAM-SA, were synthesized via free radical polymerization. The compounds required for synthesizing both NIPAM and -NIPAM-SA can be classified broadly into three major groups: Monomers, Crosslinkers and Initiator. The monomers for the synthesis used were N-isopropylacrylamide (NIPAM, 97%), sodium acrylate (SA, 97%), the crosslinker used was Ammonium per sulphate N, N′-methylenebisacrylamide (MBA, 99%)**,** while the initiator used was ammonium persulfate (APS, ≥98.0%)**.** All compounds used were purchased from Sigma Aldrich and were handled and stored according to best practices and standards recommended by the supplier.

The objective of the first synthesis was to become familiar with the synthesis process as described by literature and to build confidence in the knowledge of the process. NIPAM-SA was chosen as the first hydrogel to be synthesized via free radical polymerization. The following apparatus were used in the synthesis alongside the required monomers, crosslinker and initiator; Beakers, Capped bottles, Volumetric flask, Deionized water, Measuring scale, protective gloves and protective glasses and laboratory coat.

2.2 General Synthesis Procedure

The synthesis procedure followed to synthesize both NIPAM and NIPAM-SA are reported here. The steps are based of inference from steps followed by Razmjou et al. (2013). Firstly, for the synthesis of NIPAM-SA, an equimolar ratio (1:1) of SA and NIPAM monomers was dissolved in deionized water at room temperature in a capped bottle to form 16.7 wt.% solution. After the complete dissolution of the monomers, 0.057 g of N,N′-methylenebisacrylamide cross-linker was added to the monomer solution. Polymerization was then initiated by adding 0.04 g of ammonium persulfate into the solution at 70 °C. The hydrogel Sample was then kept at 70℃ overnight to ensure complete polymerization. The obtained hydrogels were immersed daily into fresh deionized water, for a few days, before drying at 80℃ in a convection oven to remove any possible un-crosslinked oligomers or any unreacted reactants. For the synthesis of NIPAM, the same procedure was followed but the difference here been, NIPAM was the only monomer used in the synthesis, as against an equimolar ratio of NIPAM and SA used for the synthesis of NIPAM-SA[6]. Figure 2 shows a schematic diagram depicting a summary of the steps undertook to achieve synthesis of both NIPAM and NIPAM-SA.

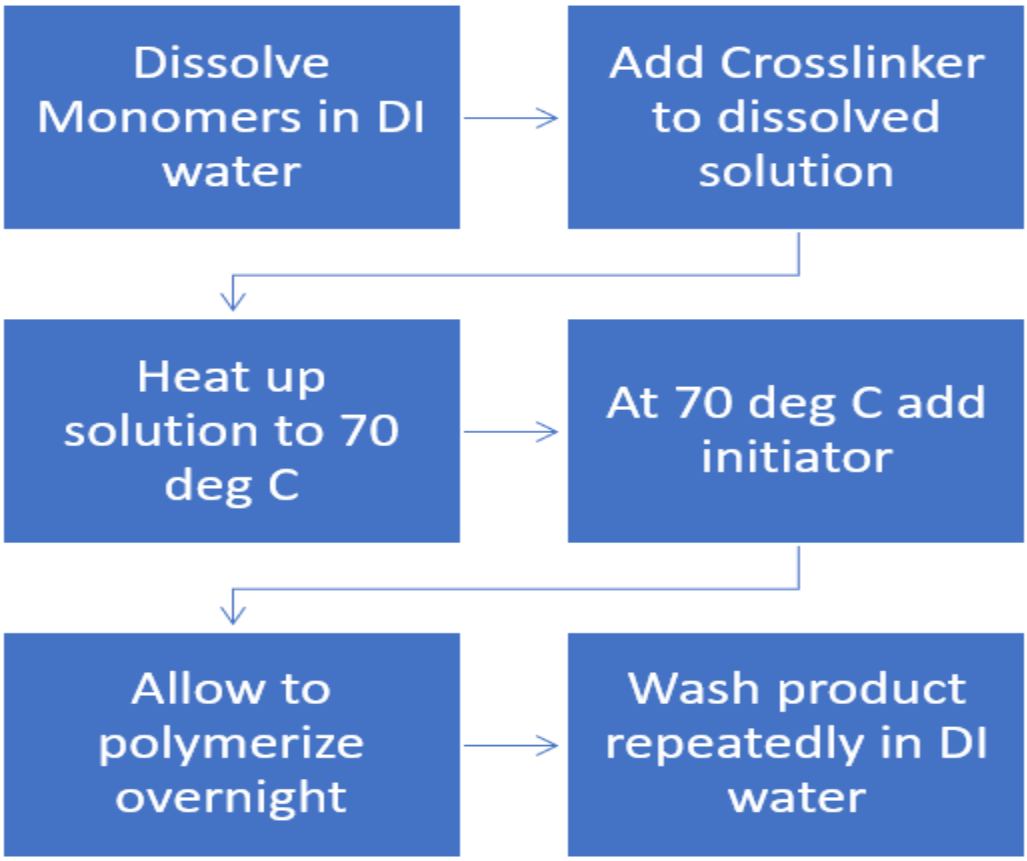

Figure 2: Schematic diagram of general synthesis procedure

2.3 Experimental Setup for First Synthesis Of NIPAM-SA

For the first synthesis, which involved the synthesis of NIPAM-SA via free radical polymerization, a simple setup as can be seen from figure 3 was used. It included a Haake water bath to help attain and maintain a polymerization temperature of 70°C, a closed flask to contain the compound diluted with deionized water, thermocouples connected to an Omega data acquisition system, and a computer to visually monitor temperature and record readings from the data acquisition hardware. Figure 4 provides a more detailed depiction of how the individual components of the experimental setup were connected to each other.

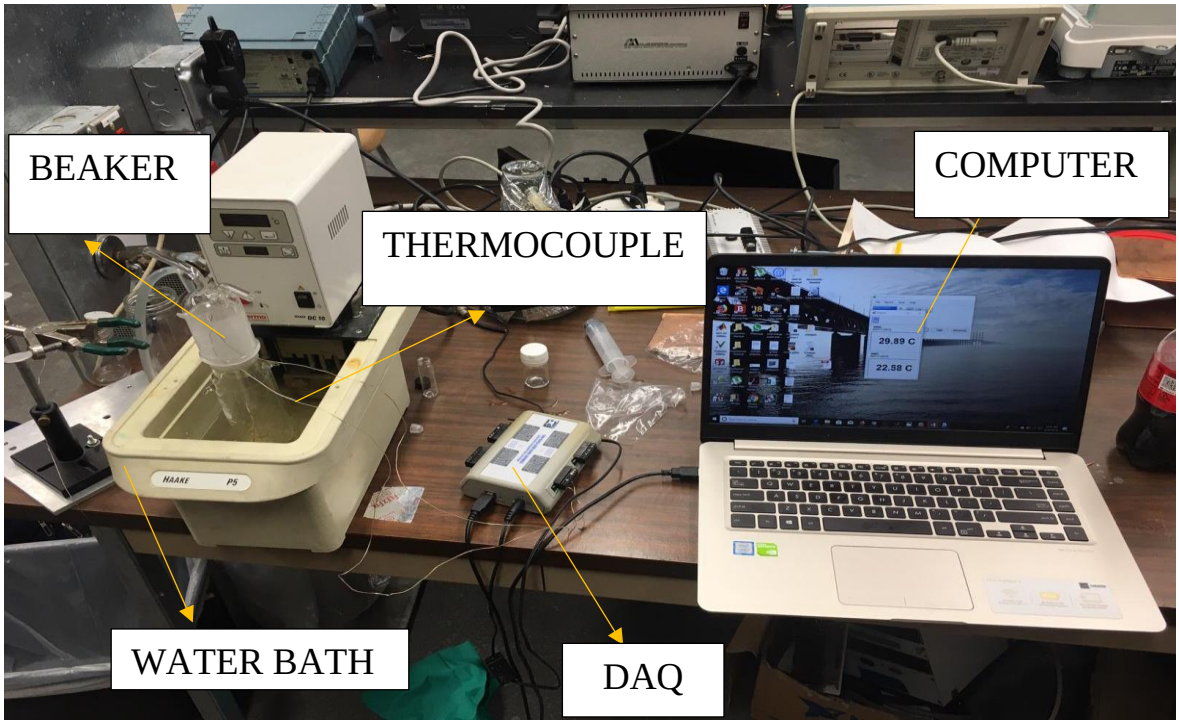

Figure 3; Experimental setup of first synthesis environment for the synthesis of NIPAM-SA. A water bath, data logger, closed flask, thermocouples and computer can be seen connected to synthesize and monitor polymerization temperature.

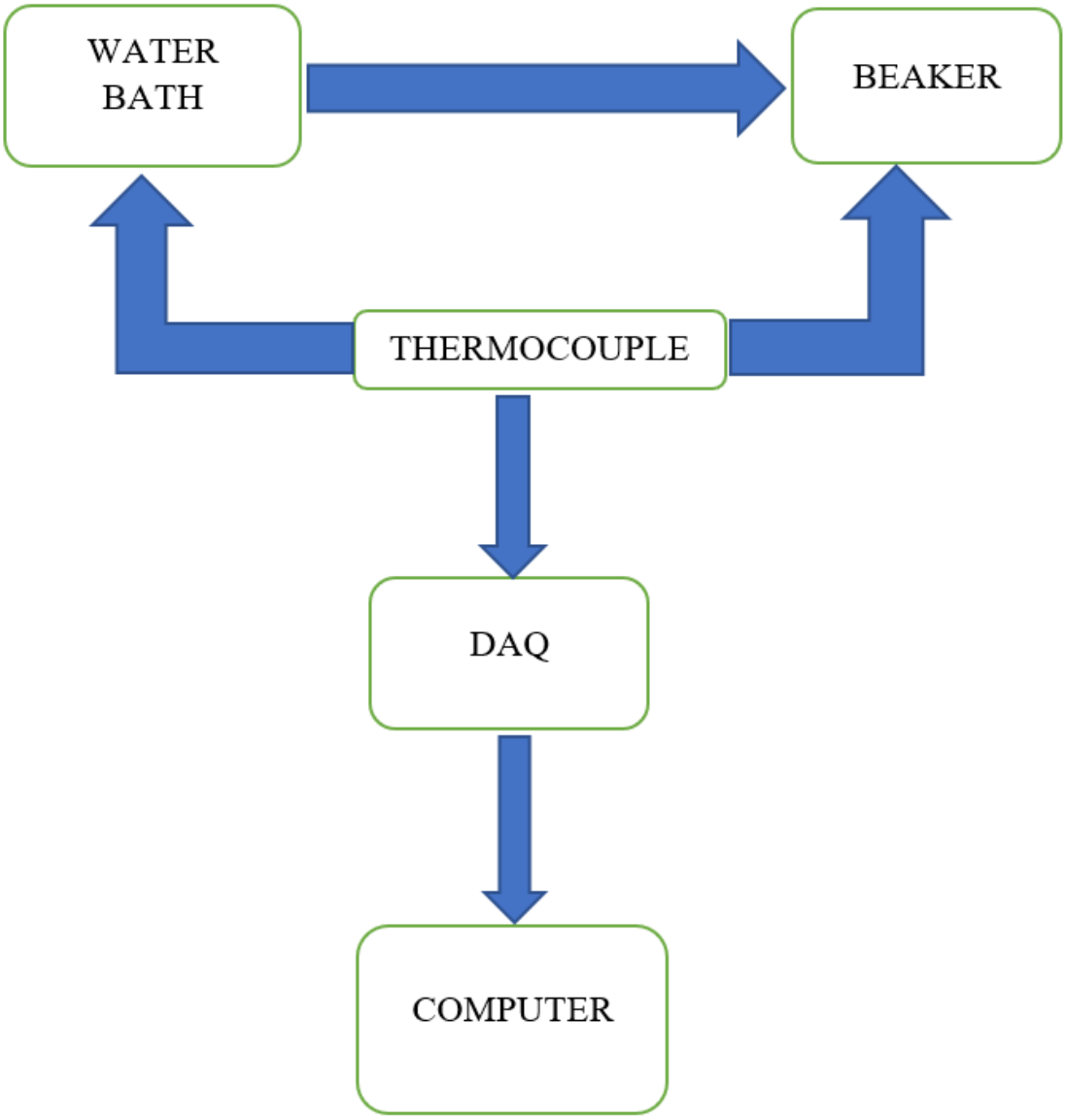

Figure 4: Schematic of experimental setup for first synthesis of NIPAM-SA. This synthesis was performed in regular atmosphere

Although care was taken to minimize exposure of the diluted compounds to oxygen, it must be mentioned that this synthesis was not performed in an inert atmosphere. Literature reports that there is an advantage to synthesizing in an inert atmosphere, as the presence of oxygen may prevent complete polymerization [6]. Figure 5 shows an image of the output product from the first synthesis. It can be seen to have taken the shape of the cross section of the round bottom flask it was synthesized in.

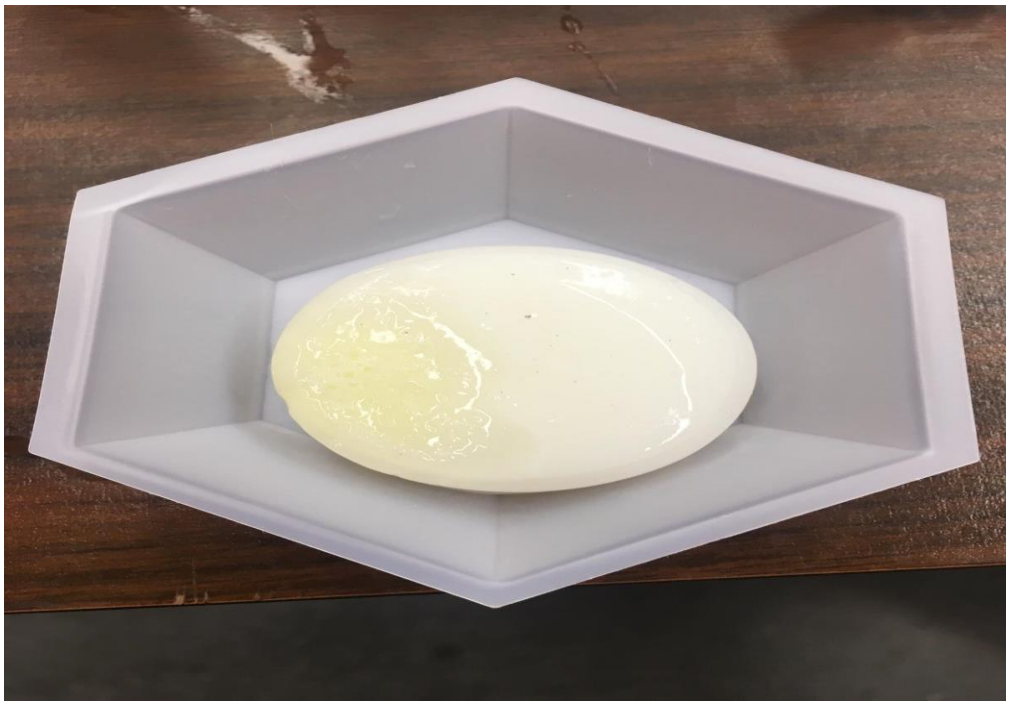

Figure 5: NIPAM-SA produced from first synthesis. For perspective on the size of the hydrogel, the inner cavity of the holding container shown here was 5mm, and the sample of hydrogel had little wiggle room when placed in it.

2.4 Synthesis of NIPAM and NIPAM-SA in An Inert Atmosphere

Recall from section 2.3 that synthesis was performed in "open air" and not without attaining an inert atmosphere. The initial synthesis environment did not have a ready supply of inert gas, hence synthesis had to be conducted in a glove box equipment courtesy of the Eyring Material's Center, Arizona State University. The glove box fitted with a ready supply of nitrogen, which is an inert gas, availed an inert atmosphere for synthesis to be conducted. The hardware setup for synthesis was similar to the setup for the synthesis in open air atmosphere, except that the Haake water bath was replaced with a hot plate heater filled with sand to serve as a thermal sink and the temperature data acquisition system was replaced with a liquid-in-glass thermometer. The glove box maintained a nitrogen atmosphere while polymerization was taking place and allowed access to the box to adjust temperature settings or adjust placement of beakers without running the risk of contaminating the inert atmosphere. Figure 6 shows a pictorial view of the glovebox setup, showing the sand heating system and the separate jars of NIPAM and NIPAM-SA. Figure 7 provides a schematic diagram showing the connections of the individual components of the experimental setup,

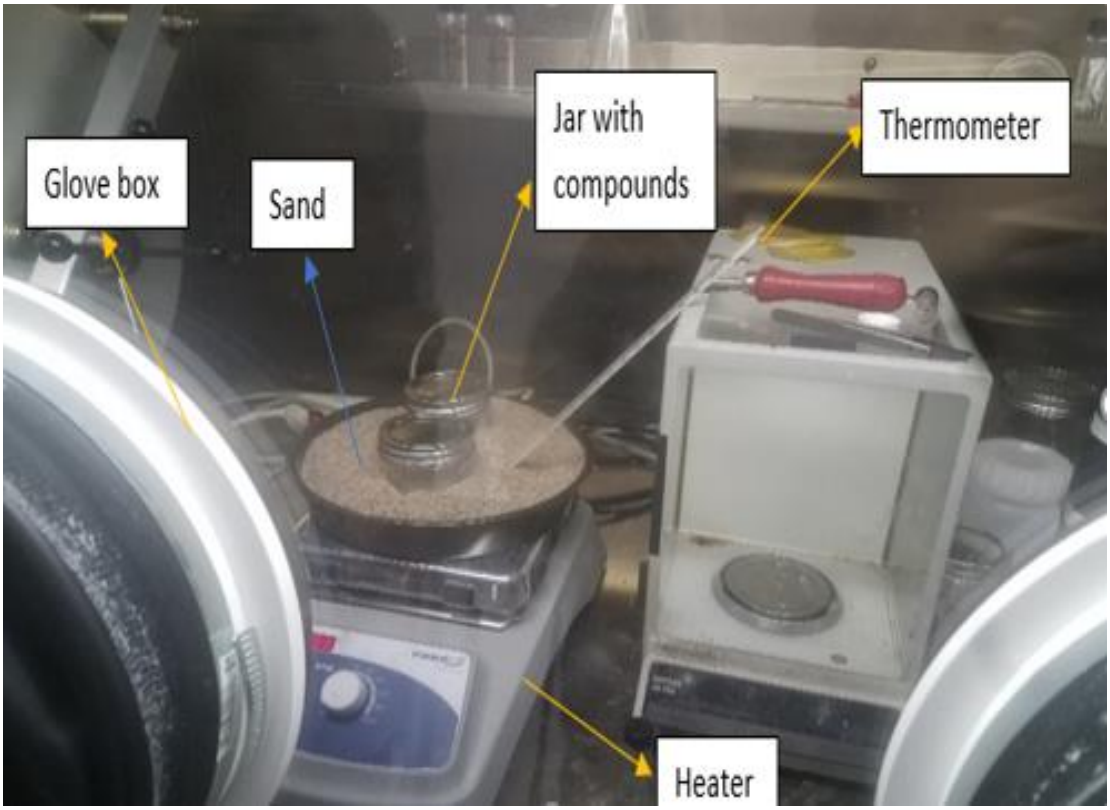

Figure 6: Experimental setup inside glovebox, with a flow of nitrogen gas maintaining inert atmosphere.

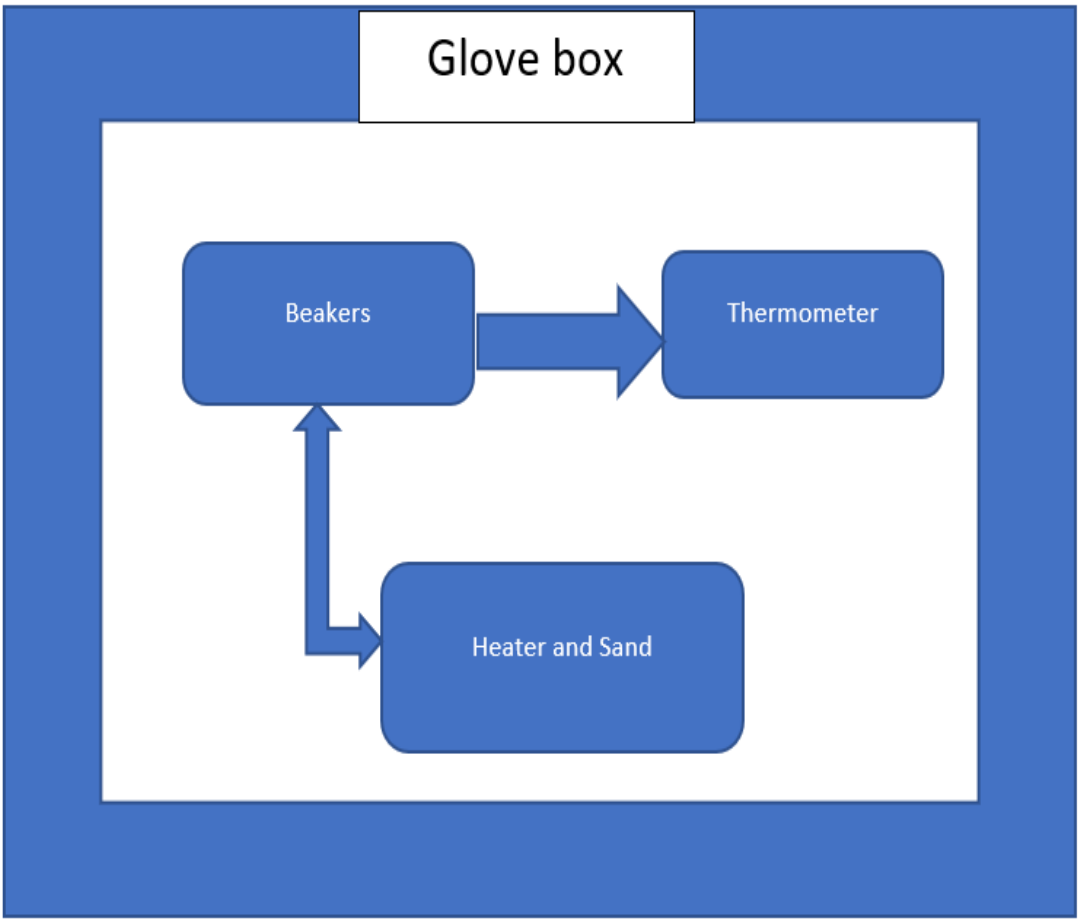

Figure 7: Schematic diagram showing the connection of the individual components of the experimental setup of the inert atmosphere synthesis of NIPAM and NIPMA-SA

2.5 Validation of Hydrogels Synthesis Via Swelling Ratio Comparison

The swelling ratio of the synthesized hydrogel is perhaps the most important parameter to be measured, as it determines how much of an osmotic pressure the hydrogel can generate, ergo how efficient it will be in FO desalination. For this work, it was crucial to use the information obtained about the swelling ratios of the hydrogels to ascertain the validity of the synthesis procedure undertook. This test shed light on whether there was any gain in synthesizing in an inert atmosphere, and if the addition of a hydrophilic ionic group like Sodium Acrylate to NIPAM really had a positive effect on the swelling ratio as suggested by reference literature [6].

This test involved studying gravimetrically the mass gain of dry samples of both NIPAM and NIPAM-SA immersed in room temperature water, as a function of time. Swelling ratio as the name implies is the ratio of the mass change in the given hydrogel sample when immersed in a fluid over a given period, to the original dry weight of the sample:

$$SW = \frac{(M_s(t) - M_D)}{M_D} \quad (1)$$

From equation 1, we see that swelling ratio (SWR) is time dependent as the mass of wet hydrogel M_s varies as time evolves.

The experimental setup for this test involved a digital scale balance, dry samples of both NIPAM and NIPAM-SA, and a stopwatch for accurate recording of the time the samples were immersed in water. Results of these tests are presented in Chapter 3.

2.6 Validation of Hydrogels Synthesis Via LCST Tests

The LCST of hydrogels particularly the class of hydrogels under study which are thermoresponsive is of key importance as regards to not only their suitability as draw agents in terms of energy required to recover draw agent but can also serve to validate synthesis. For this study, LCST reference points of 32-34℃ and ~80℃ are the expected LCST for NIPAM and NIPAM-SA respectively [7][6].

To investigate this predicted behavior, the experimental setup consisted of applying temperature stimuli to both samples and ascertain their gravimetric response at relevant temperature values. The constant heat supply was provided by a *Haake* water bath, and the internal temperature of the gel samples was confirmed with thermocouples carefully placed in the gels. A scale balance alongside a timer was used to ascertain water loss as time evolved, and results from the experiment performed on both NIPAM and NIPAM-SA are available in Chapter 3. Figure 8 and figure 9, provide a pictorial view of the setup used for the test on both NIPAM-SA and NIPAM respectively. It must be mentioned that there is a unique difference as to how NIPAM-SA and NIPAM were tested for this study, albeit great similarity in their experimental setup. The difference being that in the case of NIPAM-SA, a swollen sample of NIPAM-SA was immersed in a beaker containing water at regulated temperatures, and its weight was monitored as temperature increased to ascertain the equivalent temperature when its weight gain would become insignificant and the sample would begin to shrink. While for NIPAM, the swollen sample was placed in a dry jar, which was then heated by a water bath over a range of pertinent temperature values while tracking water loss.

Figure 8; Experimental setup for NIPAM-SA LCST investigation.

Figure 9: Experimental setup for NIPAM LCST investigation

2.7 Setup of FO Desalination Experiments

Desalination experiments were performed using synthesized NIPAM and NIPAM-SA individually in a homemade cell along with a cellulose triacetate flat sheet membrane. The objective of this round of experiments was to measure FO performance of synthesized hydrogels comparatively to obtainable results in published literature.

Of relevance to this work are the permeation flux and dewatering flux performance of the synthesized hydrogels. To this effect, and for ease of comparison a 2000-ppm salt solution, same as used in reference literature (Razmjou et al et al. 2013) was used as the feed solution. A water-tight glass jar with a sizeable circular opening in the top allowing for placement of FO membrane was used, as can be seen in figure 11. The FO cell assembly consisting of the membrane-covered glass jar and particulate hydrogel samples placed on top were placed on top a hotplate stirrer, whose only role was to provide the stirring motion to avoid accumulation of salt close to the membrane. This assembly/arrangement is depicted in figure 12 [9]. The glass jar serving as the homemade FO module, was carefully chosen due to its partial open top for ease of membrane placement and the slight offset it gives when closed that allows the feed water to always be in contact with the membrane. For an initial test of the homemade FO cell module, a dry sample of NIPAM-SA, depicted in figure 10 was placed atop the module to ascertain if permeation and hence swelling of the dry sample would occur. Figure 11 provides a view of the homemade FO cell, with a sample of NIPAM-SA that transitioned from its dry state to the swollen state atop it.

Figure 10: 0.9103g of dry NIPAM-SA

Figure 11: glass jar used as homemade FO cell module under testing. NIPAM-SA sample atop CTA membrane swelled to 5.0809g after a 48hr period, from a dry weight of 0.9103g

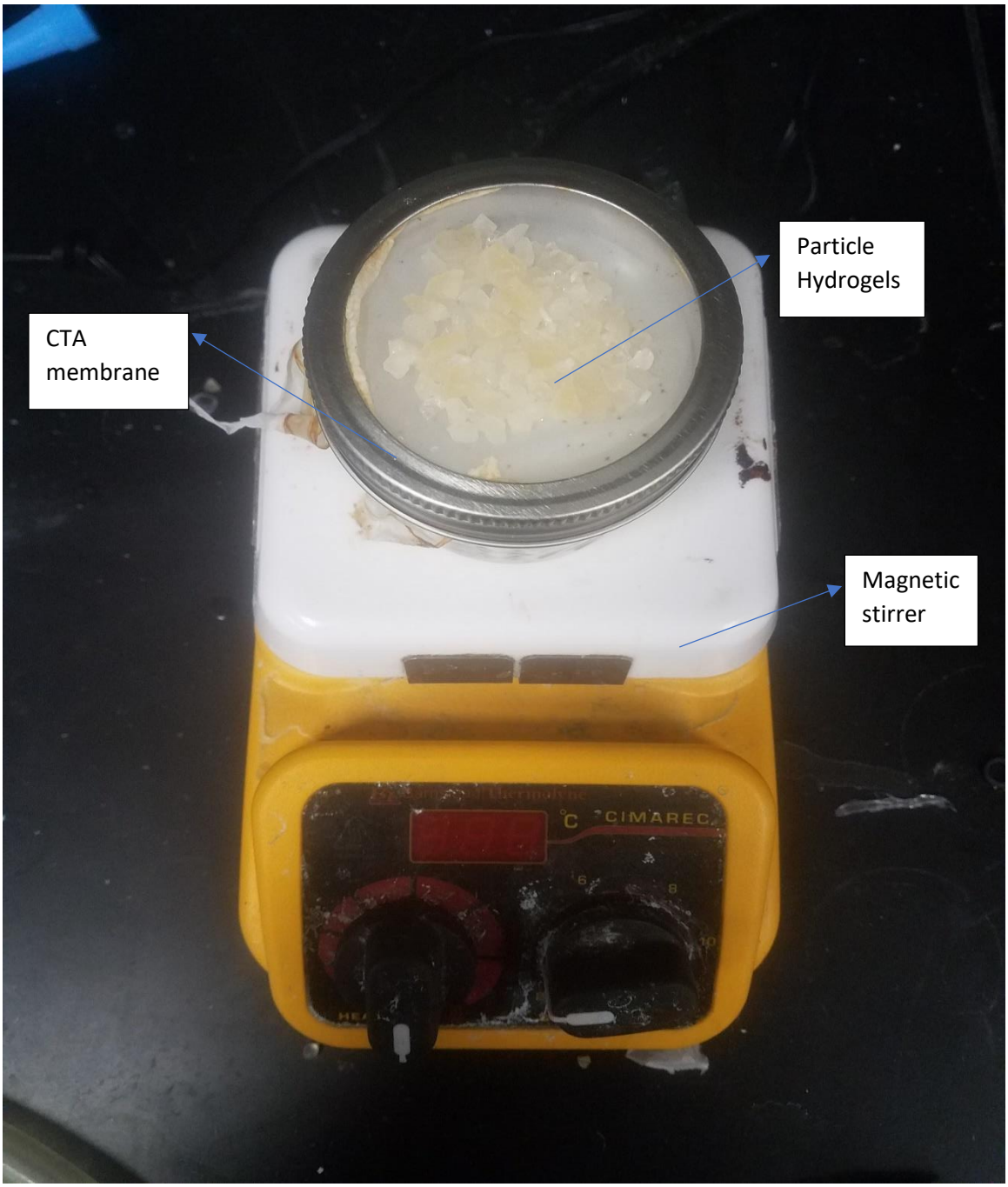

Figure 12: Setup of desalination experiment with a layer of particle hydrogels on membrane.

2.8 Setup of Vapor adsorption test on NIPAM-SA

The liquid absorption capabilities of NIPAM are well established and documented in literature. However, very little is known about its vapor adsorption capabilities. Due to NIPAM'S relatively low LCST, if found suitable for adsorption, it could be further leveraged as an adsorbent for adsorption cooling systems.

NIPAM-SA, attained by the introduction of the highly hydrophilic ionic group Sodium acrylate into NIPAM, proved to be a greater absorber of liquid as compared to NIPAM, and hence it was hypothesized that perhaps it would yield more impressive adsorption rates than NIPAM as well. The experimental setup consisted simply of a humidifier to generate water vapor, a compressed air supply, and an accumulation chamber where the flow of air and vapor could mix. An Arduino based temperature and humidity sensor was used to ensure that relative humidity stayed between 80-90℃ at all times. The sample of NIPAM-SA was placed in a test bed which was also linked to the accumulation chamber. A gravimetric approach was used to ascertain the percentage by mass of vapor adsorped by the sample. Figure 13 provides a pictorial description of the test setup and the interconnections between individual elements.

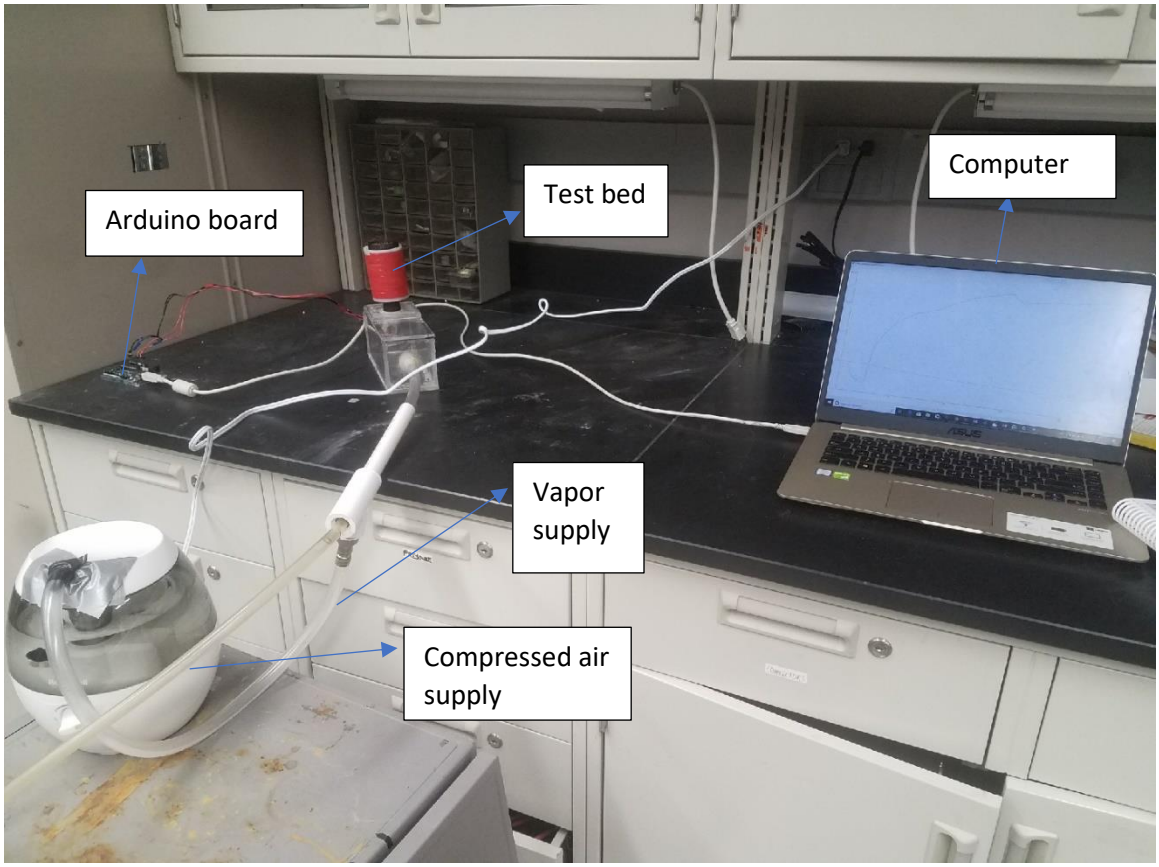

Figure 13: Vapor adsorption experimental setup

CHAPTER 3

RESULTS AND DISCUSSION

3.1 Swelling Ratio Comparison Of NIPAM-SA's Synthesized in Different Atmospheres

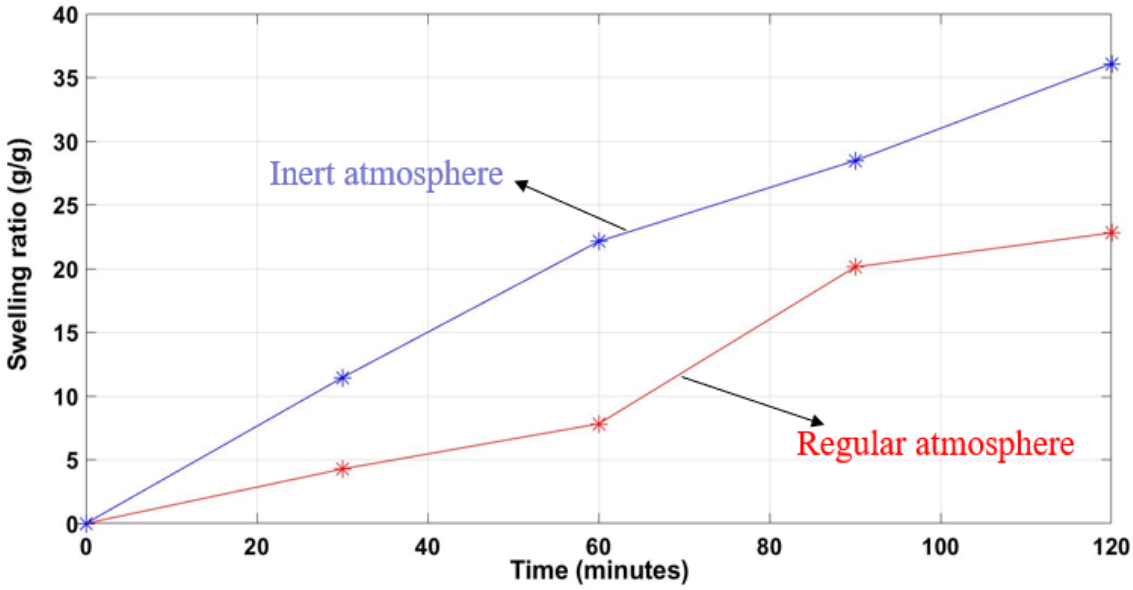

Figure 14: This graph shows the comparison of the swelling ratios of two samples of NIPAM-SA synthesized under inert atmosphere and regular atmosphere respectively. The test was performed at room temperature of 23℃.

The test for which figure 14 represents, was performed by simple immersion of the samples in room temperature water of 23℃. The NIPAM-SA synthesized in the glove box with flowing nitrogen at the atmosphere, clearly outperformed the product synthesized in the regular atmosphere as indicated by the disparity in swelling ratios over the same time interval. The synthesis conducted in the purge box performed better due to the fact that polymerization proceeded completely and was not hindered by oxygen as was the case for the synthesis conducted in regular atmosphere with oxygen present.

3.2 Swelling ratio Comparison between NIPAM and NIPAM-SA

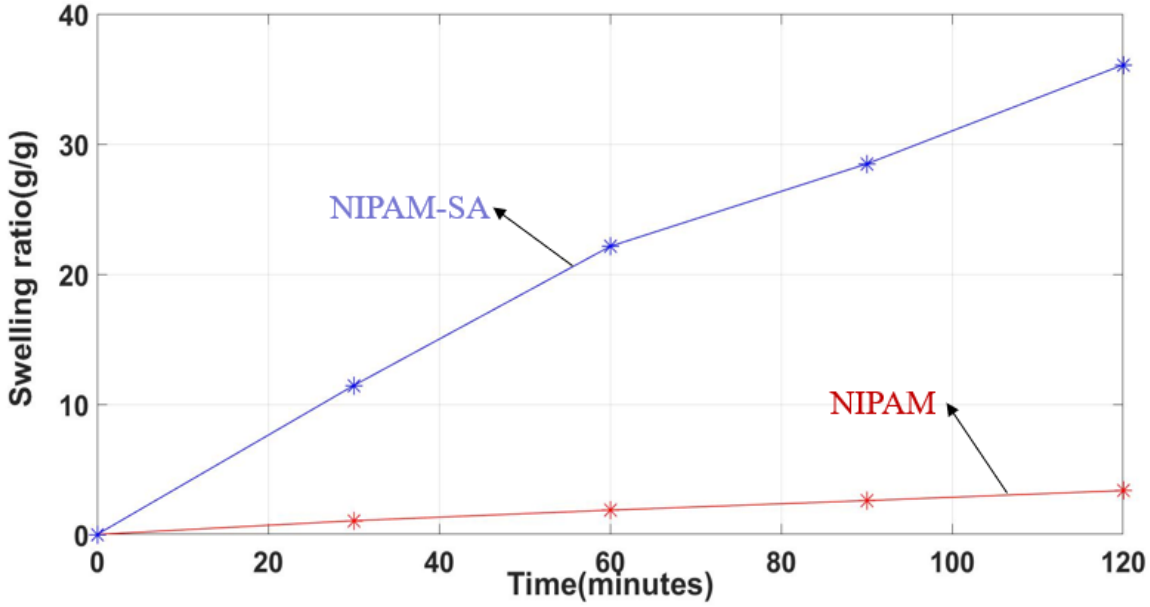

Figure 15: This graph shows the comparison between swelling ratios of NIPAM and NIPAM-SA over time. Both samples were synthesized in an inert atmosphere glove box, with flowing nitrogen as the gas supply.

NIPAM-SA, due to the introduction of the hydrophilic ionic group of Sodium Acrylate, performed better as expected in terms of swelling ratio than NIPAM performed. It is interesting to see the huge disparity in performance over time between NIPAM-SA and NIPAM in terms of swelling ratio. This result provides backing to Ramzjou et al (2013) claim that NIPAM-SA could generate flux greater than NIPAM, and this feature made it suitable to serve as the absorptive layer for a proposed novel bi-layer hydrogel driven FO desalination system.

3.3 LCST Test for NIPAM

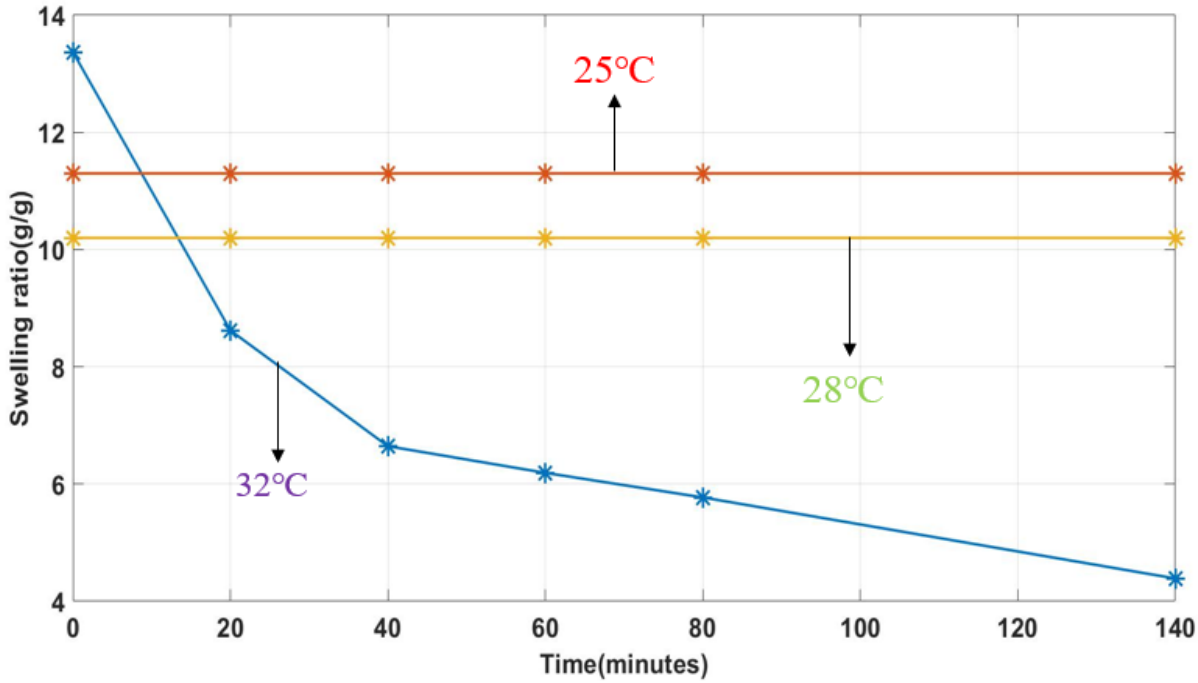

Figure 16 ;This graph shows the dewatering profile of NIPAM at the predicted LCST temperature of 32 degrees Celsius, and at temperatures approaching LCST, such as 25°C and 28°C

It is observed, as indicated by the graph, that water is lost rapidly in the first 20 minutes, then less rapidly as time evolves. This is consistent with the general reported behavior of NIPAM in literature[6][9][10]. The test was also performed at temperatures below LCST of NIPAM such as at 25 °C and at 28 °C, with no notable change in mass recorded. The graph shows different starting points in terms of swelling ratios, because different samples were used which all possessed unique individual initial swelling rations.

3.4 LCST Test for NIPAM-SA

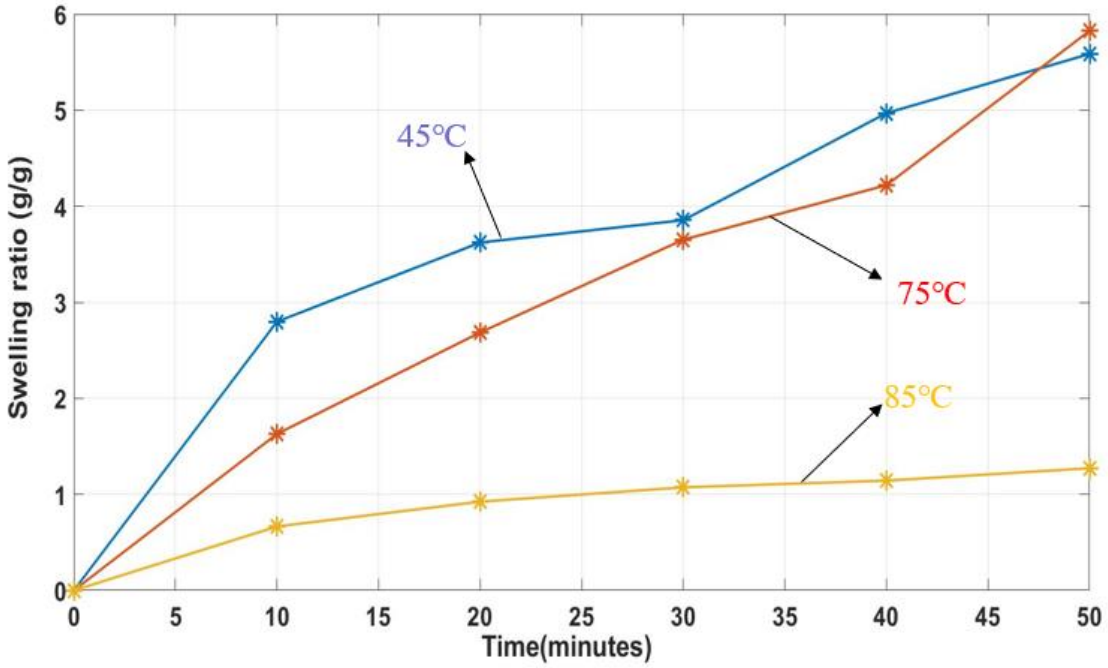

Figure 17; Presented here, is the result from the LCST test performed on NIPAM-SA at temperatures of 45°C, 75°C and 85°C.

NIPAM-SA has a comparatively greater LCST temperature than NIPAM, which literature reports to be ~ 80°C [7]. This test differs uniquely from LCST test conducted on NIPAM, as a swelling test (sample immersed in fluid as depicted by figure 8) at temperatures 45°C, 70°C, 85°C was performed to investigate its swelling behavior at key temperatures. It is seen that the swelling performance reduces drastically with increase in temperature, and this is more significantly as the sample is immersed in fluid in the region of its LCST at 85°C.

3.5 Desalination Results

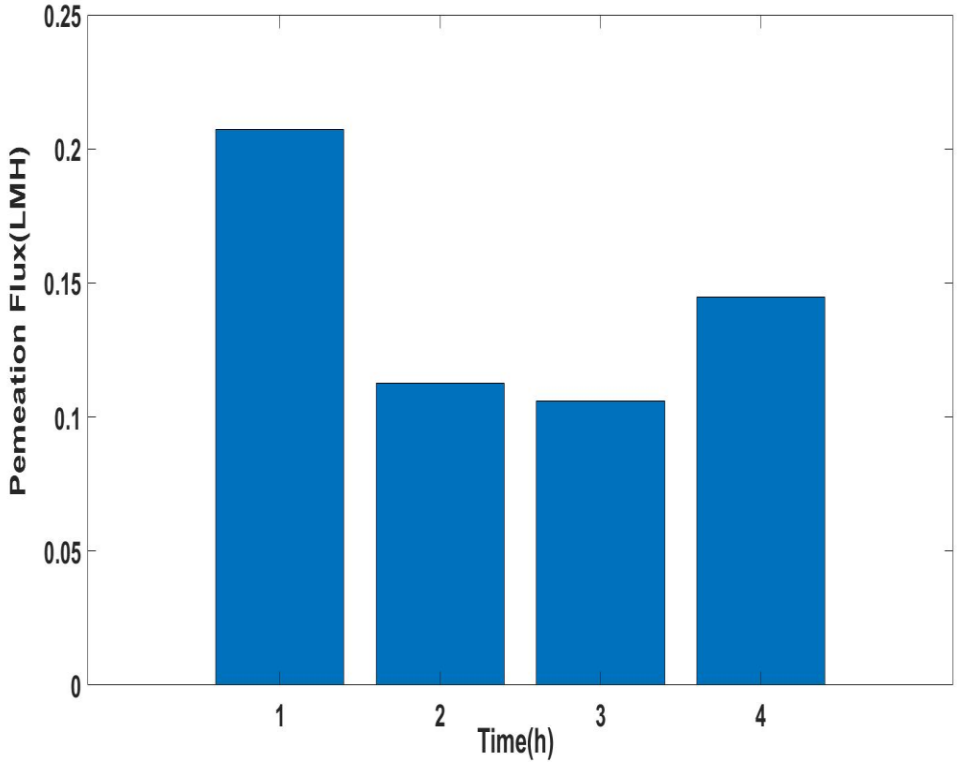

Figure 18: Presented here is the permeation flux for a sample (particle) of dry NIPAM-SA with mass 0.95695g, spread over an area of 1.5386cm^2. Permeation experiment was conducted over a period of 4 hours with a feed solution of 2000ppm prepared salt solution.

As can be seen the average permeation flux generally decreased as time evolved. Ramzjou et al. (2013) reports a decreasing trend in permeation flux with a single layer of NIPAM-SA. Ramzjou et al. (2013) reports a permeation flux peak of ~ **0.25L.m^{-2}.h^{-1}**, and a low of **~0.13L.m^{-2}**.h^{-1}.Comparatively, studies conducted in this work presents a peak permeation flux **0.2072 L.m^{-2}.h^{-1}**, and a low of **~0.1060L.m^{-2}.h^{-1}**.

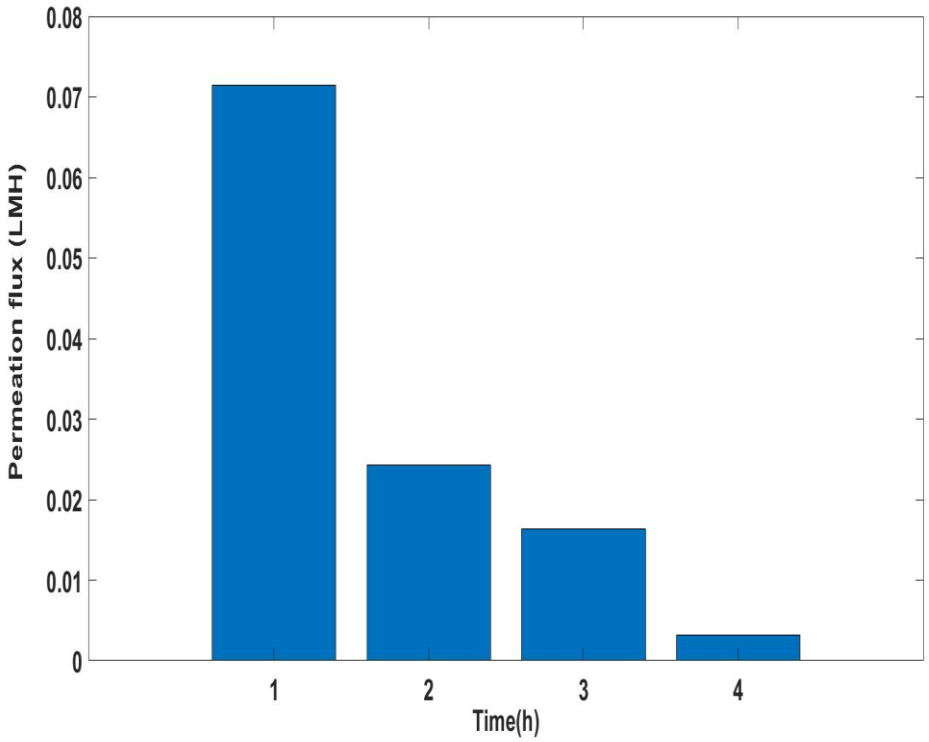

Figure 19: Presented here is the permeation flux for a sample (particle) of dry NIPAM with mass 0.8662g, spread over an area of 1.5386cm^2. Permeation experiment was conducted over a period of 4 hours with a feed solution of 2000ppm prepared salt solution.

As can be seen the average permeation flux generally decreased as time evolved. Razmjou et al (2013) reports a decreasing trend in permeation flux with a single layer of NIPAM. Amir et al (2013) reports a permeation flux peak of **~0.14L.m^{-2}.h^{-1}**, and a low of **~0.052L.m^{-2}.h^{-1}**.Comparatively, studies conducted in this work presents a peak permeation flux **0.07L.m^{-2}.h^{-1},** and a low of **0.0032L.m^{-2}.h^{-1}**.

3.6 Result of Vapor Adsorption Test on NIPAM-SA

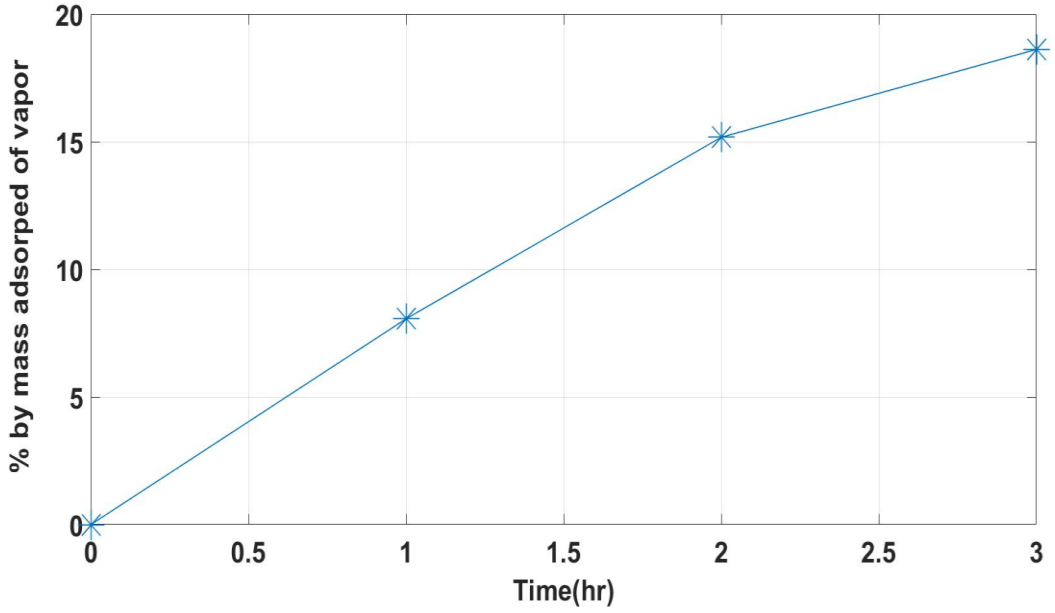

Figure 20: Presented here is the percent by mass of adsorped vapor by NIPAM-SA against time for a period of 4 hours.

The results obtained are not as impressive as expected, and when compared to liquid absorption performance of NIPAM-SA, which absorbed over 300% of its mass in liquid over a 2-hour period from swelling test depicted in figure 14 (at 45°C) , the conclusion of poor performance is easy to reach. Further studies on adsorption, especially in the context of Thermoresponsive hydrogels are needed to fully understand and improve the adsorption potential of NIPMA-SA.

CHAPTER 4

COCNLUSIONS AND FUTURE WORKS

4.1 Conceptual Hydrogel Driven FO Design

The low permeation flux by generated by NIPAM and NIPAM-SA layers, and even with a bilayer arrangement using a thin layer of NIPAM-SA as the absorptive layer due to its greater osmotic pull and a layer of NIPAM as the dewatering layer, is abysmal compared to a conventional FO draw agent such as ammonium bicarbonate, which can generate flux ~10LMH for saline solutions comparable to sea water(0.5M NaCl solution)[12]. Studies on the suitability of hydrogels as draw agents ultimately propose designs modelled around either a flat sheet membrane or a hollow fiber membrane. Razmjou et al (2013) proposed a semi batch hydrogel driven system modelled around a flat-sheet membrane with a solar concentrator delivering the energy input. Yufeng et al (2013) proposed a waste heat driven system modelled around a hollow fiber membrane, coated with semi-IPN hydrogels as draw agents.

For any proposed concept, a system of temperature control must be established, to achieve the alternation between ~ room temperature and relevant LCST temperature. For the concept proposed by this work, an indoor bi layer design inspired by Razmjou et al (2013), leveraging the unique properties of both NIPAM-SA (high swelling ratio) and NIPAM (low LCST) is recommended alongside a hollow fiber membrane. The feed solution passes through the hollow fiber membrane and the bilayer arrangement of Thermoresponsive NIPAM and NIPAM-SA generate osmotic pressure to perform desalination. Temperature is proposed to be controlled by a relay, a temperature controller connected to the

dewatering layer of the bilayer hydrogel arrangement and a DC powered heat supply. Since the idea is for the proposed design to be an indoor "home module", the DC powered heater can be connected with the battery supply of a home's solar power system. Figure 21 shows a flowchart summarizing the proposed concept.

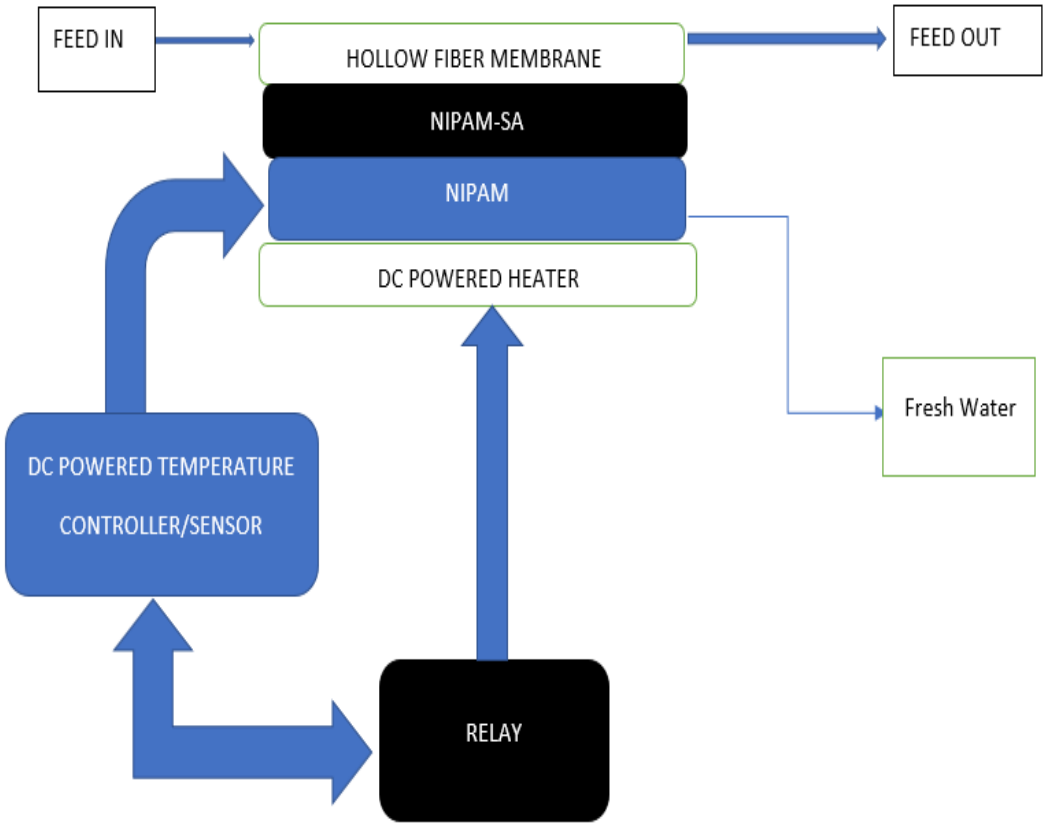

Figure 21: Schematic representation of key components of proposed conceptual bilayer hydrogel driven FO desalination system. Except for the energy require to pump feed water through the system, the actual dewatering of the NIPAM layer would be provided by a DC power source, preferably a battery linked to a home solar power system.

4.2 Energy Requirement for NIPAM layer Dewatering

It is crucial to be able to ascertain the energy requirement of any proposed design that requires the use of thermoresponsive hydrogels as draw agents. Ultimately, for hydrogel-driven FO systems, the matter simplifies to an evaluation of the energy required to cause a reversible volume phase transition at the LCST temperature. The minimum energy required to achieve a breakdown of the NIPAM layer and hence dewatering serves as the guideline for comparison with other membrane-based processes.

Perhaps, a better understanding of the mechanism of water release in NIPAM would aid in the understanding of the underlying governing thermodynamic equations that evaluates the minimum required energy. When NIPAM experiences a temperature above its LCST, PNIPAM chains receive energy to rearrange bound water into free water, and to cause association of hydrophobic segments of PNIPAM changes to force the release of water [6]. Figure 22 describes the volume phase transition process and the corresponding associated energy requirement for each stage.

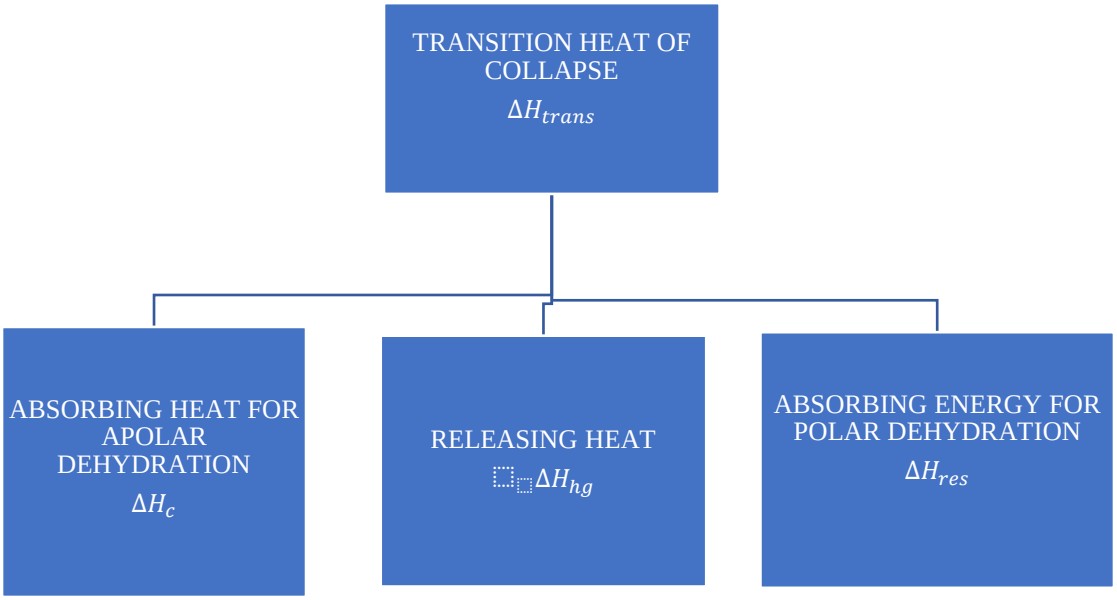

Figure 22: Breakdown of the energy components of the volume phase transition of NIPAM

The absorbing heat for apolar dehydration (ΔH_C) is due to the restructuring of water cages to bulk water around the NIPAM polar region, the absorbing energy for polar dehydration (ΔH_{hg}) is due to the rearrangement of water molecules around the amide group to form bulk water, while the releasing heat (ΔH_{res}) is a result of the intermolecular interaction between PNIPAM residues.[6]

$$\text{Hence:} \quad \Delta H_{trans} = \Delta H_C + \Delta H_{hg} - \Delta H_{res} \tag{2}$$

Reference literature gives the values of $\Delta H_C = 7.9 kJ/mol$, $\Delta H_{hg} = 17 - 22.6 kJ/mol$, ΔH_{res}=-22.6KJ/mol[6][10]. Hence given the ranges, we can deduce ΔH_{trans} = 2.3-7.9KJ/mol , and based on the molar mass of NIPAM (113.6g/mol) , we can deduce a range of 20.25-69.54kJ/kg_{PNIPAM} as against 20.25-64.26kJ/kg_{PNIPAM} reported in Ramzjou et al., which appears to be an arithmetic error on the author's part. Hence, averaging both

extremes yields a value of $44.90kJ/Kg_{PNIPAM}$ as against $42.25kJ/Kg_{PNIPAM}$ reported by the author [6].

It is worth noting that practically the energy required to deswell hydrogel is greater than the minimum theoretical energy due to portions of the energy being stored by free water. This however can be significantly reduced when the released water, which is at the same temperature as the LCST, is used to preheat the feed water. The energy stored by the free water is given by eqn (3) below. It accounts for the specific heat capacity of water (C_p) with value $4.18\mathrm{J/g℃}$, a difference in temperature(ΔT)of $7℃$ signifying a temperature rise in the water from room temperature of $25℃$ to the hydrogel LCST temperature of $32℃$, and the mass of water present (m) obtainable by the product of the swelling ratio of the hydrogel (Q) and the dry mass of hydrogel (m_h).

$$q = mC_p\Delta T = Qm_hC_p\Delta T \qquad \text{eqn (3)}$$

Ultimately, eqn (4) presented below provides an accounting of all energies require for the release of water from a given sample of swollen hydrogel.

$$w = q + m_h\Delta H_{trans} \qquad (4)$$

The energy stored by the feed water can be used for the preheating of subsequent swelling cycles. Assuming perfect heat transfer, and hence raising the temperature of the feed water through preheating results in ΔT bcoming reasonably small and hence a drastic reduction in q . Preheating the feed water with free water from collapse of the hydrogel results in the energy stored by the free water becoming negligible and hence eqn (4) can be simply resolved to eqn (5), given below.

$$w \sim m_h \Delta H_{trans} \quad (5)$$

For context and to provide a baseline for comparison of the energy requirements of more established desalination technologies, a NIPAM sample with a dry mass of 1g would require between 0.02kJ-0.07kJ for liberation of free water. Taking into account the quantity of water liberated which is a product of the swelling ratio and the dry mass of hydrogel, the energy required translates to 4-14kJ/kg as against the 4-12.8kJ/kg reported by Ramzjou et al (2013). This value obtained translates to $1.11-3.9 kWhr/m^3$, as compared to 2.2 $kWhr/m^3$ at which well optimized RO plants operate [11]. This comparison also must be put in the context that most RO plants operate at a recovery of 50% as compared to the unrealistic assumption that 100% water recovery is attained when NIPAM collapses.

4.2 Conclusion and Future Works

Despite the low permeation flux values recorded in this work, which is consistent with obtainable values in literature, hydrogels still represent a fascinating alternative for draw agents due to their membrane friendliness, water compatibility, and in the case of NIPAM, low LCST. A bi-layer arrangement as put forth by Razmjou et al (2013) presents great promise, if a means of drastically increasing permeation flux to values at least comparable with conventional draw agents such as ammonium bi carbonate, can be developed. Future endeavors should investigate what mechanism could perhaps allow for drastic improvement in permeation flux. Although current literature favors the investigation of possible materials that could be blended with NIPAM, perhaps more effort should be placed on physical processes that could increase permeation flux, such as the introduction of ultrasound. This work has studied the synthesis and characterization of both NIPAM and NIPAM-SA and used them to perform desalination individually, with obtained results comparable to published data by Razmjou et al (2013). Furthermore, a conceptual design for a novel home friendly DC powered desalination module using a bilayer arrangement of hydrogels has been proposed.

REFERENCES

[1] Charette, Matthew A., and Walter HF Smith. "The volume of Earth's ocean." *Oceanography* 23.2 (2010): 112-114

[2] Bhojwani, S., Topolski, K., Mukherjee, R., Sengupta, D., & El-Halwagi, M. M. (2019). Technology review and data analysis for cost assessment of water treatment systems. *Science of the Total Environment*, *651*, 2749-2761

[3] Chandwankar R.R., Nowak J. (2019) Thermal Processes for Seawater Desalination: Multi-effect Distillation, Thermal Vapor Compression, Mechanical Vapor Compression, and Multistage Flash. In: Lahnsteiner J. (eds) Handbook of Water and Used Water Purification. Springer, Cham

[4] Ibrahim, G. S., Isloor, A. M., & Yuliwati, E. (2019). A Review: Desalination by Forward Osmosis. In *Current Trends and Future Developments on (Bio-) Membranes* (pp. 199-214). Elsevier.

[5] Li, Z., Linares, R. V., Sarp, S., & Amy, G. (2018). Direct and Indirect Seawater Desalination by Forward Osmosis. In *Membrane-Based Salinity Gradient Processes for Water Treatment and Power Generation* (pp. 245-272). Elsevier.

[6] Razmjou, A., Liu, Q., Simon, G. P., & Wang, H. (2013). Bifunctional polymer hydrogel layers as forward osmosis draw agents for continuous production of fresh water using solar energy. *Environmental science & technology*, *47*(22), 13160-13166.

[7] Hirotsu, S., Hirokawa, Y., & Tanaka, T. (1987). Volume-phase transitions of ionized N-isopropylacrylamide gels. *The Journal of chemical physics*, *87*(2), 1392-1395.

[8] Ahmed, E. M. (2015). Hydrogel: Preparation, characterization, and applications: A review. *Journal of advanced research*, *6*(2), 105-121

[9] Zeng, J., Cui, S., Wang, Q., & Chen, R. (2019). Multi-layer temperature-responsive hydrogel for forward-osmosis desalination with high permeable flux and fast water release. *Desalination*, *459*, 105-113.

[10] Cho, E. C.; Lee, J.; Cho, K. Role of bound water and hydrophobic interaction in phase transition of poly(N-isopropylacry9929-lamide) aqueous solution. Macromolecules 2003, 36 (26),9934.

[11] Li, C., Goswami, Y., & Stefanakos, E. (2013). Solar assisted sea water desalination: A review. *Renewable and Sustainable Energy Reviews*, *19*, 136-163.

[12] McCutcheon, J. R., McGinnis, R. L., & Elimelech, M. (2005). A novel ammonia—carbon dioxide forward (direct) osmosis desalination process. *Desalination*, *174*(1), 1-11.

APPENDIX A

MATLAB CODES

```
t=[0 20 40 60 80 140]

dw=133.3647*ones(1,6)

NW=[142.4782 139.2406 137.8943 137.5841 137.2982 136.3558]

size(NW)

size(t)

consize=132.6831*ones(1,6)

gamma= 11.3*ones(1,6)

alpha=10.2*ones(1,6)

RW=NW-consize

Rdw= dw-consize

for i=1:6
DWr(i)= (RW(i)-Rdw(i))/(Rdw(i))
end
plot(t,DWr,'LineWidth',2,'Marker','*')
hold
plot(t,gamma,'LineWidth',2,'Marker','*')
plot(t,alpha,'LineWidth',2,'Marker','*')


%bar(t,DWr)
```

```
tg= [1 2 3 4 ]

% dw=133.3647*ones(1,6)
NW=[ 0.9565 1.0216 1.0570 1.0903 1.1358]
size(NW)
% size(t)
%consize=1.6038*ones(1,6)
%RW=NW-consize
% Rdw= dw-consize
for i=1:4
DWr(i)= ((((NW(i+1)-NW(i))/1000 )/1000)* 1000)/(3.142*0.010^2)
% *(t(i+1)-t(i)))
end
%plot(t,DWr,'LineWidth',2,'Marker','*')
bar(tg,DWr)
tg= [1 2 3 4 ]

% dw=133.3647*ones(1,6)
NW=[ 2.470 2.5598 2.5904 2.611 2.615]
size(NW)
% size(t)
consize=1.6038*ones(1,5)
%RW=NW-consize
 Rdw= NW-consize
for i=1:4
DWr(i)= ((((Rdw(i+1)-Rdw(i))/1000 )/1000)* 1000)/(3.142*0.02^2)
% *(t(i+1)-t(i)))
end
%plot(t,DWr,'LineWidth',2,'Marker','*')
bar(tg,DWr)
```

APPENDIX B

DSC RESULTS FOR NIPAM AND NIPAM-SA

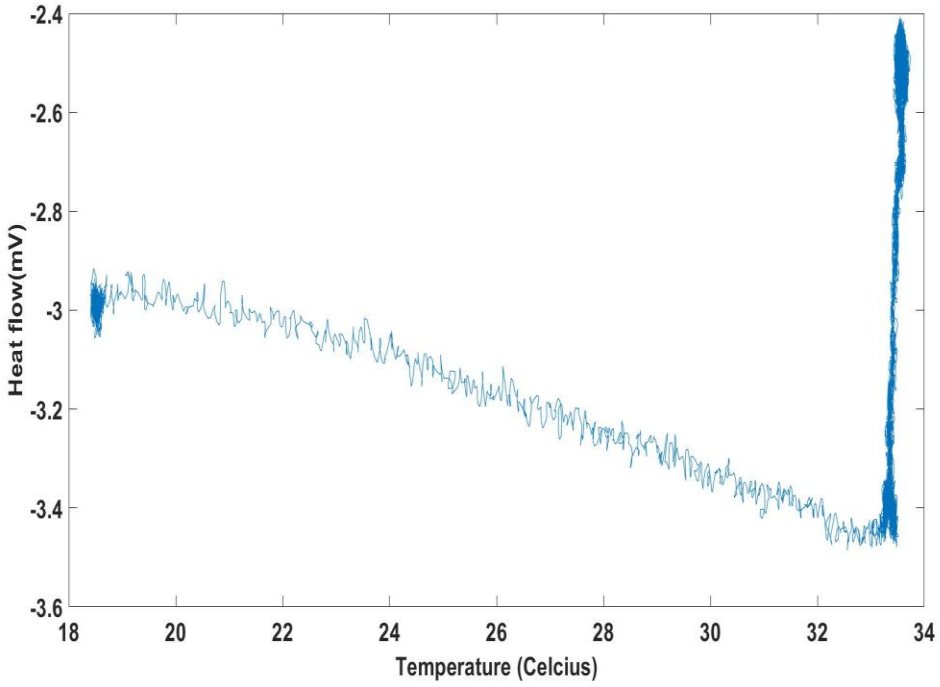

DSC results for NIPAM showing phase transition between 32-33℃

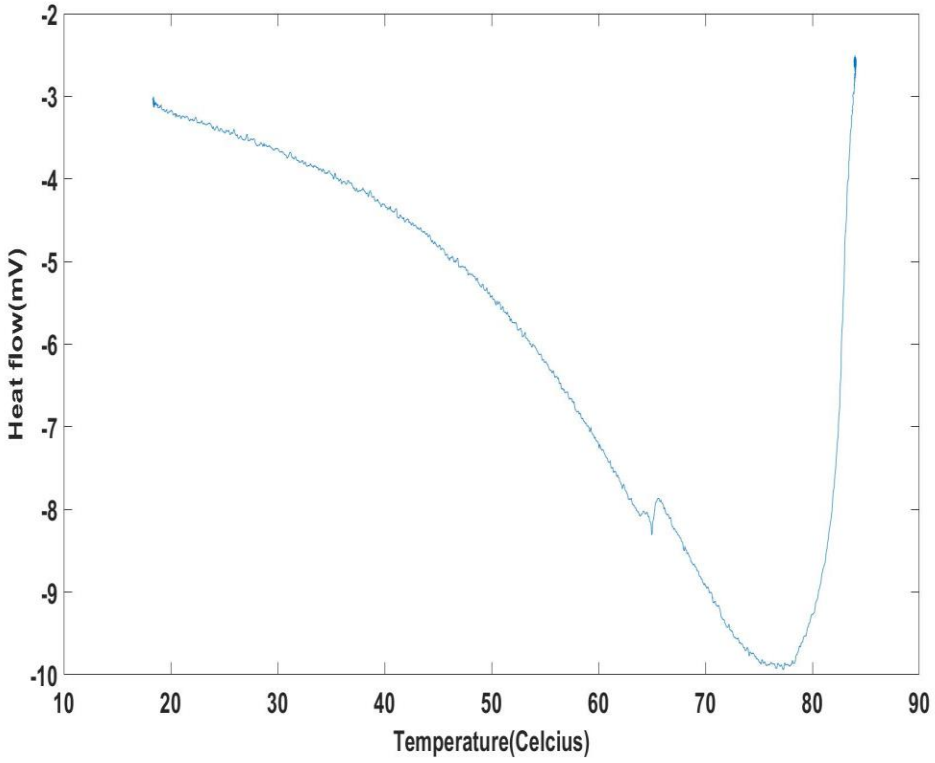

DSC results for NIPAM-SA showing phase transition between 71-80℃